

# Temperature dependence of optical anisotropy of holographic polymer-dispersed liquid crystal transmission gratings

I. Drevenšek-Olenik,<sup>1,2</sup> M. Fally,<sup>3</sup> and M. A. Ellabban<sup>3,4</sup>

<sup>1</sup>*Faculty of Mathematics and Physics, University of Ljubljana, Jadranska 19, SI 1001 Ljubljana, Slovenia*

<sup>2</sup>*Department of Complex Matter, J. Stefan Institute, Jamova 39, SI 1001 Ljubljana, Slovenia*

<sup>3</sup>*Nonlinear Physics Group, Faculty of Physics, University of Vienna, Boltzmannngasse 5, A-1090 Vienna, Austria*

<sup>4</sup>*Physics Department, Faculty of Science, Tanta University, Tanta 31527, Egypt*

(Received 21 April 2006; published 21 August 2006)

We measured the angular dependence of the 0th,  $\pm 1$ st, and  $\pm 2$ nd optical diffraction orders from a  $50\ \mu\text{m}$  thick transmission grating recorded in a UV-curable holographic polymer-dispersed liquid crystal (HPDLC) made from commercially available constituents. The analysis was performed for two orthogonal polarizations of the probe beams. The emphasis was laid on the temperature dependence of the grating anisotropy. Above the nematic-isotropic phase transition, the grating is optically isotropic. At lower temperatures the grating strength for the optical polarization perpendicular to the grating vector decreases with decreasing temperature, while for orthogonal polarization it increases with decreasing temperature. As a consequence, a regime of diffraction with strongly overmodulated gratings is observed. Our investigations indicate that the anisotropy of the refractive-index modulation scales with the optical anisotropy of the liquid crystal medium forming the phase-separated domains. We further demonstrate that light scattering effects, which are profound only in the nematic phase, must not be neglected and can be taken into account via a Lorentzian line-shape broadening of the probing wave vector directions in the framework of the diffraction theory for anisotropic optical phase gratings.

DOI: [10.1103/PhysRevE.74.021707](https://doi.org/10.1103/PhysRevE.74.021707)

PACS number(s): 61.30.Pq, 42.25.Fx, 42.70.Ln, 64.70.Md

## I. INTRODUCTION

Holographic polymer-dispersed liquid crystals are electrically switchable photonic media with large potential for applications in devices such as optical interconnects, beam steering elements, lenses with switchable focus, mirrorless lasers, image capture elements, and various kinds of reflective flat panel display devices [1–11]. They are fabricated by photopolymerization of a mixture of photocurable monomers and liquid crystal (LC) in the interference field of two or more laser beams. During the initial stage of photopolymerization, inhomogeneous illumination causes the monomers to diffuse to bright and the LC molecules to diffuse to dark regions of the optical interference pattern. When some specific level of polymerization is reached, unmixing of the components takes place, resulting in formation of phase-separated LC domains which are periodically distributed in the polymer network [12–15]. Investigations by scanning electron microscopy (SEM) show that, depending on the composition of the mixture, kinetics of the phase separation process and the periodicity of the optical pattern, holographic polymer-dispersed liquid crystal (HPDLC) gratings exhibit a wide range of morphologies, from a well-defined stack of alternating planes of LC-rich regions (in the form of LC planes, spongelike LC regions, or LC droplets) separated by layers of a pure polymer, up to a three-dimensional (3D) interconnected porous network that hardly reveals any noticeable spatial periodicity [16–25].

Despite a broad diversity of their morphologies, practically all HPDLCs are strongly optically anisotropic. For transmission gratings the diffraction efficiency is usually much larger for polarization perpendicular to the LC-rich planes ( $p$  polarization) than for polarization along the LC-

rich planes ( $s$  polarization) (see Fig. 1) [21,26–44]. For structures with a droplet morphology this property is related to the elongated shape of the LC droplets, which in combination with appropriate surface anchoring leads to the nematic director field with preferred direction perpendicular to the holographic planes [12,45,46]. For structures exhibiting nondroplet morphologies the alignment of LC is explained by a scaffolding effect of the polymer network, which is attributed to planar anchoring of the LC at the surface of polymer filaments present in the LC-rich regions [4]. On the contrary, in the recently discovered sliced gratings (POLIC-RYPS) the alignment is ascribed to homeotropic anchoring of the LC molecules at the LC-polymer interface [47–50]. Therefore no general rule regarding the alignment and the associated anisotropy seems to exist. Besides this it was

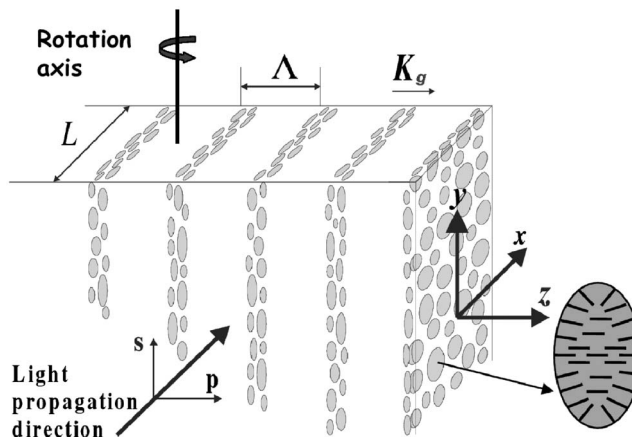


FIG. 1. Schematic drawing of the HPDLC transmission grating.

shown experimentally that even when using the same polymer compound, alternation of the LC compound and/or modification of the glass substrates can drastically change the polarization dependence of diffraction properties [51].

Characterization of HPDLC structures is typically performed on samples with a thickness of about  $10\ \mu\text{m}$  and a grating spacing of around  $1\ \mu\text{m}$ . The optical diffraction efficiency is usually measured at a fixed orientation of the grating with respect to the probe beam. The incident angle of the probe beam is selected so that the diffracted beam has maximal intensity, which in general is assumed to correspond to the Bragg angle. However, due to the extremely large refractive-index modulation of the HPDLC media this assumption might be wrong. Even at such relatively small sample thickness the grating strength can be overmodulated, leading to considerably reduced diffraction at the Bragg angle. The term overmodulation signifies that due to the energy exchange between the transmitted and the diffracted beams the amplitude of the diffracted wave is reduced by the backflow of energy into the transmitted wave. Consequently, the modulation is actually larger than assumed and maxima of the diffraction efficiency can appear far off the Bragg angle [52]. On the other hand, in  $10\ \mu\text{m}$  thick samples the conditions for thick Bragg gratings are often not fulfilled, so that the conventional analysis based on two-wave coupling theories might be doubtful [53]. These problems can lead to various misinterpretations, which can be avoided only by performing a thorough angular analysis of the diffraction properties around the Bragg angle.

An additional complication arising in HPDLC systems is the presence of diffuse light scattering, which appears due to random size and orientation of the phase-separated LC domains [54]. The diffuse scattering can be accompanied also by holographic scattering (HS), which is generated by diffraction from parasitic gratings formed during the photopolymerization process [55]. These features cause additional difficulties in evaluating the refractive-index modulation from the measured values of the diffraction efficiency.

To resolve the origin of the optical anisotropy of gratings recorded in HPDLC and to elucidate some of the above-mentioned complications in determining their basic optical parameters, we performed a systematic study of the diffraction properties of UV-curable transmission gratings made from commercially available constituents. The emphasis was laid on the temperature dependence of the grating anisotropy. At each investigated temperature we measured a complete angular dependence (i.e., the so-called rocking curve) of the intensities of the 0th,  $\pm 1$ st, and  $\pm 2$ nd diffraction orders. The measurements were performed for  $p$ - as well as for  $s$ -polarized probe beams. The obtained data were analyzed in the framework of the theories of Kogelnik or Montemezzani and Zgonik (MZ) for light propagation in isotropic and in anisotropic optical gratings, respectively [56,57]. The scattering effects, which are profound only in the nematic phase, were taken into account via a Lorentzian line-shape broadening of the probing wave vector directions in the MZ theory. As a convenient simplification we found that, particularly in case of overmodulated gratings, the grating strength parameter can be evaluated quite accurately by considering only the positions of the minima in the rocking curve instead of fitting the entire curve.

## II. EXPERIMENTS

### A. Sample preparation

We used a material composition similar to that reported in the literature [4,58]. The samples were prepared from the UV curable emulsion containing 55 wt % of the LC mixture (TL203, Merck), 33 wt % of the prepolymer (PN393, Nematel), and 12 wt % of the 1,1,1,3,3,3-hexafluoroisopropyl acrylate (HFIPA, Sigma-Aldrich). Standard cells made from two glass plates separated by  $d=50\ \mu\text{m}$  thick Mylar spacers were filled with the optically isotropic mixture by means of the capillary flow. The samples were cured in the interference field of two expanded beams from an argon ion laser operating at a wavelength of  $\lambda_{UV}=351\ \text{nm}$ . The writing beams entered the sample symmetrically with respect to the sample normal, so that an unslanted transmission grating with the grating spacing of  $\Lambda=1.2\ \mu\text{m}$  was recorded. The total intensity of the  $s$ -polarized writing beams was  $6\ \text{mW}/\text{cm}^2$  (Fig. 1). Holographic exposure time varied between 10 and 40 s. After holographic recording the samples were postcured by illumination with only one of the two writing beams. The postcuring times were in the range from 90 to 120 s. According to our previous experience these were about the optimal conditions to obtain stable gratings with a high overmodulation of the diffraction efficiency and a suitable level of diffuse scattering. All the samples had rather similar optical properties. To perform a detailed analysis of the temperature dependence of the diffraction features we selected the sample which was recorded for 35 s and postcured for 105 s. This sample was afterward analyzed also by dynamic light scattering (DLS) and SEM. The angular width of the diffraction peaks was probed by the sample that was recorded for 13 s and postcured for 120 s. All the samples, which were postcured for 90 s and more, were optically stable for several months, while for lower postcuring times the diffraction intensities decreased by sample aging in the time scale of days. The sample postcured for 105 s was selected for detailed optical analysis also because it was previously studied by small angle neutron scattering (SANS), which will be reported in a separate paper.

The TL203 nematic liquid crystal mixture used for our gratings has a positive optical anisotropy with  $n_a=n_{||}-n_{\perp}=0.201$ , where  $n_{\perp}=1.529$  is the ordinary and  $n_{||}=1.730$  is the extraordinary refractive index. Consequently, the refractive index in the isotropic phase is expected to be  $n_I\sim\langle n_{LC}\rangle=1.599$ . The TL LC compounds are composed of pentyl cyanobiphenyl (5CB) mixed with fluoro- and chloro-substituted mesogens [1]. The bulk nematic-isotropic (NI) phase transition of TL203 is at  $77\ ^\circ\text{C}$ . The prepolymer system PN393 is an ethylhexyl acrylate based mixture with a refractive index  $n_p=1.473$ . The fluoro-additive (HFIPA), which is presumed to mediate anchoring properties at the polymer-LC interface [23], has the refractive index  $n_F=1.319$ . All data are given for  $\lambda=589\ \text{nm}$ .

### B. Analysis of the diffraction properties

The sample was mounted to a heating stage, the temperature of which was controlled with an accuracy of  $\pm 0.2\ ^\circ\text{C}$ .

The heating stage was placed on a precise rotation stage with its rotation axis parallel to the  $y$  axis of the grating (Fig. 1). Diffraction properties of the sample were probed by a He-Ne laser beam with the wavelength of  $\lambda=543$  nm and an optical power of  $P=1$  mW. The beam was expanded with a collimator, after which it passed a pinhole with the diameter of 2 mm and then it was sent to the sample. Three silicon photodiodes were used to simultaneously detect the intensity of the transmitted beam (0th diffraction order) and the intensities of the two selected diffracted beams. The photosensitive area was circular with an acceptance angle of around  $\Theta=2^\circ$ .

To measure the angular dependence of the diffracted light at a fixed incident angle of the probe beam with respect to the sample, one of the photodiodes was mounted on a goniometric arm which was rotated around the sample. Also in these measurements the rotation axis was parallel to the  $y$  axis of the grating (Fig. 1), while the acceptance angle of the detector was reduced to  $\Theta=0.3^\circ$ .

To identify the NI phase transition temperature the sample was at first slowly heated from room temperature to  $T=90$  °C and the intensities of the 0th and the  $\pm 1$ st diffraction orders were measured at a fixed orientation of the sample with respect to the probe beam. In the nematic phase all the intensities strongly vary with increasing temperature, while at  $T_c=68\pm 0.2$  °C they stabilize and do not change upon further heating. We hence assume that the NI phase transition in our gratings takes place at 68 °C, which is 9 °C below the bulk transition temperature of the pure LC compound. Similar and even larger downshifts of the transition temperature are characteristic for many HPDLC systems and are attributed to the presence of prepolymer ingredients and other impurities within the LC droplets [29,47,58,59]. After identification of  $T_c$ , the angular dependence of the diffraction orders was measured at selected temperatures. In order to test for the reproducibility of the results and to rule out any possible hysteresis effects, we performed several cycles of cooling and heating between  $T=40$  °C and  $T=80$  °C. The results from various cycles were nearly identical.

### C. Structural analysis

At first we performed a nondestructive investigation of the sample structure by the DLS technique. DLS probes the dynamics of thermally induced orientational fluctuations within the LC domains. As shown in our recent paper, analysis of the DLS response provides information on the size and shape of the LC domains and on viscoelastic properties of the LC medium within the domains [58]. In PDLC and HPDLC systems the fluctuation dynamics is typically composed of two relaxation modes. The faster of them is associated with intradroplet or intrapore fluctuations and the slower with orientational diffusion of the average droplet orientation induced by irregularities of the polymer-LC interface and/or interdroplet coupling [60,61]. From the dispersion relation of the fast mode we found that the average size of the LC domains in our sample is  $0.5\times 0.9\times 0.9$   $\mu\text{m}^3$ , where the first number corresponds to the size perpendicular to the LC-rich planes, while the last two values give the dimensions parallel

to the LC-rich planes. The details of the corresponding procedure are described elsewhere [58]. Our DLS study also signifies an interconnected structure of the LC domains within the LC-rich regions, which is in accordance with the scaffolding arrangement proposed for similar formulations [4]. Both DLS modes exhibit a profoundly nonexponential relaxation dynamics, which signifies a strongly polydisperse nature of the morphological features.

To prepare our sample for the SEM imaging, one of the glass plates was detached and the grating was immersed into isopropanol to extract the LC material from the polymer network. The extraction procedure was performed in several steps. In each step the sample was at first immersed for few seconds, then isopropanol was evaporated, and after this the extraction effect was analyzed with optical polarization microscopy. Before the immersion and during the initial stages of the extraction, a profound optical birefringence of the material was detected. The two eigenpolarization directions are parallel and orthogonal to the grating vector  $\mathbf{K}_g$ , respectively (Fig. 1). By prolonged immersion the material becomes optically isotropic. Nonetheless, parallel lines associated with the grating structure are still clearly visible under the microscope and also the diffraction effects can still be observed. However, measurements of the angular dependence of the diffraction intensities show that the remaining grating is optically thin. This indicates that during the immersion procedure most of the bulk polymer network is etched away together with the LC material, so that finally only a distinct interfacial film in contact with glass plates remains. The SEM image of this remaining polymer film reveals a periodically undulated surface structure without any signs of the droplet morphology. We attribute this structure to a layer of a polymer material which is much more robust than the bulk of the HPDLC medium. It is evident that in such cases SEM does not give relevant morphological information on the HPDLC gratings. Similar experience with UV curable HPDLC materials has been reported also by other groups [4,24]. As shown recently by Hsiao *et al.*, more relevant information on the grating morphology can be achieved by using bright-field transmission electron microscopy (BFTEM) instead of the standard TEM technique [62].

## III. RESULTS AND DISCUSSION

### A. Angular dependence

Figure 2(a) shows angular dependencies of the intensity of the 0th and the  $\pm 1$ st diffraction orders measured 3 °C above  $T_c$ . The rotation angle  $\theta$  is given with respect to the normal incidence of the probe beam. The intensities are given relative to that of the incident beam, renormalized for reflection losses at normal incidence. Vertical dashed lines denote Bragg angle incidence. The results obtained for  $s$ - and for  $p$ -polarized beams are almost identical. This indicates that the grating is optically isotropic, i.e., the amplitude of the refractive-index modulation is independent of the polarization state of the optical beam.

To compensate for various kinds of optical losses, the diffraction efficiency  $\eta$  is customarily defined as the ratio between the intensity of a selected diffraction order and the

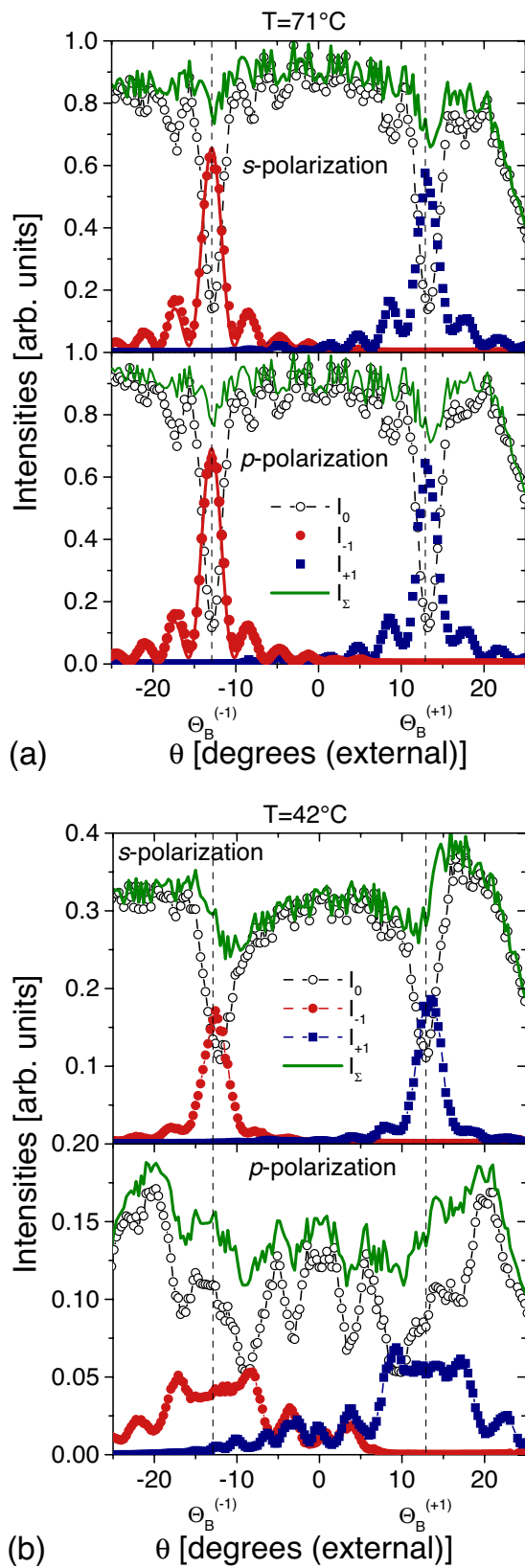


FIG. 2. (Color online) The dependencies of the 0th and the 1st order diffraction intensities on the rotation angle of the sample in the isotropic phase (a) and in the nematic phase (b). Thin solid lines in (a) are fits to Eq. (3). Vertical dashed lines denote the Bragg angle position. Note that the external angles are given.

sum of the intensities of all other diffraction orders. In our case only the nearby orders give important contributions, which means

$$\eta_{\pm 1} = \frac{I_{\pm 1}}{I_{+1} + I_0 + I_{-1}}, \quad (1)$$

where  $I_0$  denotes the intensity of the forward diffracted beam and  $I_{\pm 1}$  the intensities of the 1st order diffracted beams. Such a definition is reasonable if the denominator in Eq. (1), i.e., the sum of detected intensities  $I_{\Sigma} = I_0 + I_{-1} + I_{+1}$  is a smooth function of  $\theta$ . The values of  $I_{\Sigma}(\theta)$  are shown by thick solid lines in Fig. 2(a). One can notice that  $I_{\Sigma}(\theta)$  is relatively flat everywhere except in the Bragg angle regions, in which it experiences a dip of around 10% with respect to the average value. This suggests that optical losses are slightly larger for diffracted than for transmitted light. A strong decrease of  $I_{\Sigma}$  for  $\theta > 25^\circ$  is an artifact which appears because the incident beam was partially blocked by the walls of the heating stage.

The diffraction efficiency of a lossless isotropic volume phase grating with the thickness  $L$ , which refractive index  $n$  is described by

$$n(z) = n_0 + n_1 \cos(K_g z), \quad (2)$$

is given as [52,56]

$$\eta(\nu, \xi) = \frac{\sin^2 \sqrt{\nu^2 + \xi^2}}{1 + \xi^2/\nu^2}, \quad (3)$$

where  $\nu = \pi n_1 L / (\lambda \cos \theta)$  is the grating strength, and  $\xi = \Delta \theta \pi L / \Lambda$  is a measure for the deviation from the Bragg condition, i.e.,  $\Delta \theta = \theta - \theta_B$ . The values of  $\theta$  in these relations are associated with the beam propagation within the HPDLC medium. The Bragg angle is given by  $2n_0 \sin \theta_B = \lambda / \Lambda$ , where  $\lambda$  is the wavelength of the probe beam in free space. A fit of the experimental data shown in Fig. 2(a) to Eqs. (1)–(3) results in  $\nu_s = 1.89 \pm 0.03$  and  $\nu_p = 1.84 \pm 0.03$ , while the obtained values for grating thickness and grating spacing are  $L = 30.5 \pm 0.4 \mu\text{m}$  and  $\Lambda = 1.20 \pm 0.02 \mu\text{m}$ . The obtained value of  $L$  is 40% smaller than the thickness of the plastic spacers. Such a huge difference cannot be attributed to the shrinkage of the cell during photopolymerization. We believe that it is mainly a consequence of the formation of surface layers of pure polymer, which takes place due to hampering of the photoinitiator at the surfaces. A presence of these surface layers was revealed by the SEM analysis. The obtained value of  $n_0$  is  $1.52 \pm 0.01$ , which coincides with the average value of the refractive index calculated by simply taking into account the volume fractions of the constituents:  $\langle n \rangle = c_p n_p + c_F n_F + c_{LC} n_l = 1.524$  (for  $\lambda = 589 \text{ nm}$ ).

Figure 2(b) shows the angular dependencies of the 0th and the  $\pm 1$ st diffraction orders measured at  $T = 42^\circ \text{C}$ , which corresponds to a temperature deep in the nematic phase of the LC domains. Several profound differences with respect to the results obtained for  $T > T_c$  can be noticed. First of all the diffraction features are strongly anisotropic, i.e., the results obtained for  $s$ - and for  $p$ -polarized beams are completely different. For the  $s$ -polarized beam the shape of  $I_{\pm 1}(\theta)$  is similar as in the isotropic phase, but the maxima at  $\theta_B$  are significantly lower and the side lobes are less profound. For

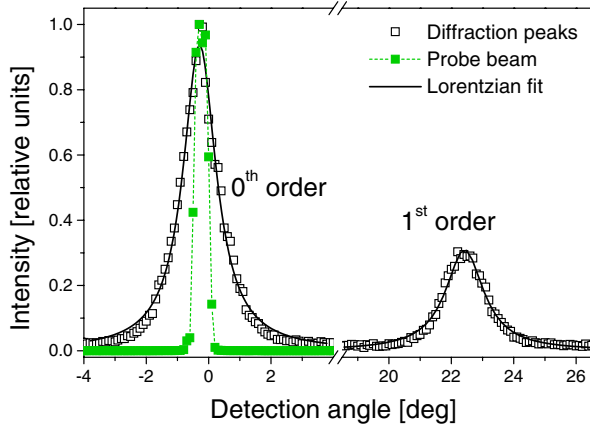


FIG. 3. (Color online) Angular dependencies of the 0th and the 1st order diffraction intensities measured by rotating the arm with the detector around the sample at a fixed orientation ( $\theta \approx \theta_B$ ) of the grating with respect to the probe beam. Solid lines are fits to the Lorentzian function. The narrow dashed line around the 0th order direction indicates the intensity measured without the sample and corresponds to the unperturbed probe beam.

the  $p$ -polarized beam double maxima appear at the side lobes, about  $5^\circ$  off  $\theta_B$ , while a near plateau is observed at  $\theta_B$ . These diffraction properties signify a strong overmodulation of the grating. We emphasize that by simply searching for the maxima of  $I_{\pm 1}$ , a determination of the Bragg angle will be completely wrong.

The second important difference with respect to the isotropic phase is that the sum of the detected intensities  $I_{\Sigma}$  is strongly reduced. For  $s$  polarization the sum intensity  $\langle I_{\Sigma} \rangle$  averaged over the angle drops to around 30% and for  $p$  polarization to around 15% of their value in the isotropic phase. This reduction is attributed to diffuse light scattering, which is strongly anisotropic as well. Diffuse light scattering is an intrinsic property of HPDLC structures, which is related to the randomness of the polymer/LC phase separation process. So far only the so-called POLICRYPS gratings were reported to show practically no diffuse light scattering [47–50], while most other HPDLC media typically exhibit quite profound light scattering phenomena.

The third difference between the nematic and the isotropic phase is that  $I_{\Sigma}$  shows strong variations with the rotation angle  $\theta$ . For  $s$  polarization the dips in  $I_{\Sigma}(\theta)$  increase to about 20% of the  $\langle I_{\Sigma} \rangle$  and are shifted from  $\theta_B$  toward  $\theta < \theta_B$ . For  $p$  polarization several minima and maxima occur which resemble the dependence of  $I_0(\theta)$ . This again signifies that attenuation is apparently stronger if optical power is redirected from the transmission to the diffraction direction. To support this explanation we measured the angular dependence of the diffracted intensities at a fixed orientation of the sample with respect to the incident beam. A result achieved for  $p$ -polarized light at  $T=25^\circ\text{C}$  and  $\theta \sim \theta_B$  is shown in Fig. 3. The corresponding diffraction peaks were fitted to Lorentzian line shapes, which resulted in the linewidths of  $\Gamma_0 = 1.29 \pm 0.03^\circ$  and  $\Gamma_{+1} = 1.45 \pm 0.04^\circ$ . Both of these values are significantly larger than the width of the unperturbed probe beam, which was  $0.5^\circ$ .

Light scattering reduces the intensities of the detected beams and for that reason it is usually considered to play a similar role as optical absorption. For isotropic gratings the effect of absorption is commonly taken into account as an exponential reduction factor in front of the Kogelnik's formula for the diffraction efficiency of a lossless grating (Eq. (3)) [35,52,54]. However, in the case of asymmetric propagation of the pump and the probe beams in anisotropic media the role of absorption in the diffraction theory becomes more complicated [57].

In contrast to absorption, light scattering produces also a broadening of the wave vector span of the propagating waves. This means that besides the diffraction of the incident beam one has to take into account also the diffraction of scattered waves. For a finite detection angle this produces a smearing of  $I(\theta)$  for all the diffraction orders. For incoherent scattering the resulting effect can be described as a superposition of the scattering intensities corresponding to a multitude of the independent plane waves.

In our samples light scattering is strongly concentrated along the forward direction, which is in agreement with relatively large size of the LC domains as revealed from the DLS measurements. At room temperature the full width at half maximum (FWHM) of the transmitted beam is 2.6 times larger than the width of the incident beam, and a central peak corresponding to the unperturbed probe beam cannot be resolved at all (Fig. 3). According to these findings we suggest a model for the diffraction efficiency which combines the optical anisotropy of the refractive index modulation with the broadening of the probing wave vector directions. As usual for HPDLC gratings, also in our case due to the symmetry, one of the eigenaxes ( $z$  axis, see Fig. 1) of the optical dielectric tensor is parallel to the grating vector  $\mathbf{K}_g$ , while the other two are parallel and perpendicular to the glass plates, respectively (Fig. 1). Therefore the optical dielectric tensor is given as

$$\boldsymbol{\epsilon} = \begin{bmatrix} \epsilon_{xx}^0 & 0 & 0 \\ 0 & \epsilon_{yy}^0 & 0 \\ 0 & 0 & \epsilon_{zz}^0 \end{bmatrix} + \begin{bmatrix} \epsilon_{xx}^1 & 0 & 0 \\ 0 & \epsilon_{yy}^1 & 0 \\ 0 & 0 & \epsilon_{zz}^1 \end{bmatrix} \cos(K_g z), \quad (4)$$

where the first term represents an average and the second a periodic modulation. If we neglect the above-mentioned difference between the apparent absorption constants of the pump and the signal waves, then the corresponding diffraction efficiency has exactly the same form as the one of Eq. (3), but with different definitions of the grating parameters for different polarizations. Namely, the corresponding relations for the  $s$ -polarized beam are [57]

$$\nu_s = \frac{\pi L \epsilon_{yy}^1}{2\lambda \sqrt{\epsilon_{yy}^0} \cos \theta_s}, \quad \xi_s = \frac{L \Delta k_s}{2}, \quad (5)$$

and for the  $p$ -polarized beam we have

$$\nu_p = \frac{\pi L(\varepsilon_{zz}^1 \cos^2 \theta_p - \varepsilon_{xx}^1 \sin^2 \theta_p)}{2\lambda \bar{n} \cos \theta_p}, \quad \xi_p = \frac{L\Delta k_p}{2}, \quad (6)$$

where  $\Delta k = |\mathbf{k}_0 - \mathbf{k}_{\pm 1} + \mathbf{K}_g|$  is a mismatch between the optical wave vectors and the grating vector. If the 0th and the  $\pm 1$ st diffraction orders experience the same refractive index, then in the vicinity of  $\theta_B$  the above given definition of  $\xi$  becomes analogous to Kogelnik's definition, i.e.,  $\xi = \Delta \theta \pi L / \Lambda$  [63]. In our experiments this approximation is reasonable, because the value of  $\theta_p$  inside the medium was always less than  $18^\circ$ . Consequently, with  $p$ -polarized light the average refractive index of the probe and the signal beams  $\bar{n}$  was always very close to  $\sqrt{\varepsilon_{zz}^0}$  and we probed predominantly the component  $\varepsilon_{zz}^1$  of the modulation. For the same reason we neglected in Eq. (6) also the terms associated with a walk-off between the wave front and the energy propagation directions.

Most of the wave vectors within the probing wave vector span  $\{\mathbf{k}_i\}$  are associated with a slightly shifted diffraction angle with respect to the unperturbed incident beam, as well as by an equally shifted sample rotation angle needed to satisfy the Bragg condition. The superposition of the corresponding scattering intensities is consequently given as

$$\eta(\nu, \xi) = \int_{-\Theta/2}^{\Theta/2} \left( \frac{\sin^2 \sqrt{\nu^2 + [\xi - \delta\xi(\alpha)]^2}}{1 + [\xi - \delta\xi(\alpha)]^2 / \nu^2} \right) f(\alpha) d\alpha, \quad (7)$$

where  $\delta\xi(\alpha) = \pi L \alpha / \Lambda$  is associated with the angular shift  $\alpha$  and  $\Theta$  is the acceptance angle of the detector. The normalized distribution of the probing wave vectors directions described by  $f(\alpha)$  is defined in a way that all the  $\mathbf{k}_i$  within the range  $f(\alpha)d\alpha$  have the same diffraction direction  $\theta_{B_i}(\alpha) = \theta_{B_0} - \alpha$ , where  $\theta_{B_0}$  is the Bragg angle for the unperturbed incident beam. Because angular broadening in the direction orthogonal to  $\mathbf{K}_g$  does affect the Bragg condition,  $f(\alpha)$  has to be calculated by reducing the corresponding two-dimensional (2D) profile of the  $\{\mathbf{k}_i\}$  to one-dimensional (1D). The resulting function can in general be quite complicated; however, in our model we take  $f(\alpha)$  with a Lorentzian line shape. The Lorentzian line shape was chosen on the basis of the measurements of angular spread of the diffracted beams (Fig. 3), which had shown that angular dependence of the diffracted peaks can be very well fitted by the Lorentzian function.

Due to the smearing effects the maxima of  $\eta(\theta)$  [defined according to Eq. (1)] are always below 1 and the minima are significantly above 0. For grating strengths  $\nu < \pi/2$ , in addition, positions of minima are shifted to the values of  $\theta$  significantly differing from the nonsmeared case. However, for  $\nu > \pi/2$  (overmodulated situations), minima for the nonsmeared and the smeared case appear nearly at the same values of  $\theta$ . This feature allows us to simplify the analysis by considering values of  $\theta$  associated with the minima of  $\eta(\theta)$  instead of fitting the entire rocking curve. The minima, which are closest to  $\theta_{B_0}$ , are most relevant. Their position on the  $\xi$  axis is given by the condition

$$\sqrt{\nu^2 + \xi^2} = N\pi, \quad (8)$$

i.e., by concentric circles with radius  $N\pi$  in the  $\nu$ - $\xi$  plane. Here  $N=1, 2, 3$  denotes the appropriate interval of  $\nu$ , namely

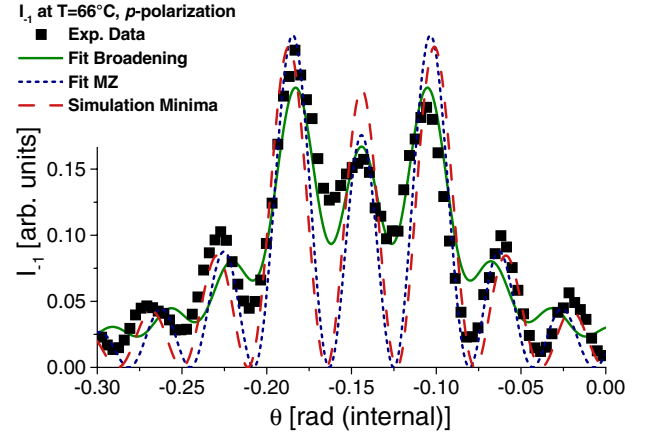


FIG. 4. (Color online) Angular dependence of the 1st order diffraction intensity for  $p$ -polarized light at  $T=66^\circ\text{C}$ . The solid line is a fit to the angular broadening model. The dotted line is a fit to the MZ theory. The dashed line is a simulation according to the MZ theory made by using the value of the grating strength as deduced from the positions of the minima in the experimental curve [Eq. (8)].

$(N-1)\pi < \nu < N\pi$ , which is resolved from comparison with other minima in the rocking curve.

The results of various fitting procedures are illustrated in Fig. 4, which shows the diffracted intensity  $I_1(\theta)$  for  $p$ -polarized light measured at  $T=66^\circ\text{C}$ . At first we calculated the value of  $\nu$  corresponding to the Lorentzian angular broadening model. The corresponding fitting curve, which shows the best agreement with the central part of the experimental data in the region of  $\theta_B$ , yields  $\nu_L=2.61$ . The obtained value of the angular spread is  $\Gamma_L=1.27^\circ$ . Then we calculated the grating strength  $\nu_m$ , which according to Eq. (8) best coincides with the positions of the minima in the measured rocking curve. From this it follows  $\nu_m=2.75\pm 0.2$ . The simulated dependence of  $\eta(\nu_m, \theta)$ , corresponding to Eq. (3) and Eq. (6), is shown as a dashed line in Fig. 4. Finally we made also a standard fit to the MZ theory which gave  $\nu_{MZ}=2.64\pm 0.2$ . In the last two cases light scattering was taken into account only as a reduction factor in front of Eq. (3). Due to the smearing effects the last two curves do not match the data in the Bragg angle region well, but their behavior in the side lobes and especially the positions of the minima with respect to the  $\theta$  axis are very close to the corresponding experimental data.

## B. Temperature dependence

For  $T < T_c$  and  $s$ -polarized light the diffraction efficiency at the Bragg angle  $\eta(\theta_{B_0})$  monotonously decreases with decreasing temperature. For a  $p$ -polarized beam, on the contrary, a profound nonmonotonous dependence is observed. This is attributed to the rapid increase of the grating strength  $\nu$ , which leads to overmodulation. An interesting feature is that on the other hand the value of  $\theta_{B_0}$  is independent of the temperature, which means that the grating pitch  $\Lambda$  does not change with decreasing temperature.

The main features are illustrated in Fig. 5(a), which shows the rocking curves observed for a set of selected temperatures. In the isotropic phase  $\eta(\theta)$  shows only one strong maximum, and the curves obtained at different temperatures are nearly identical. Below  $T_c$  side maxima start to increase, and between 67–66 °C they become higher than the central maximum. At even lower temperatures the behavior is reversed again. Most of the observed features can be explained if one plots the graphs of Eq. (3) for increasing values of  $\nu > \pi/2$ . For comparison, Fig. 5(b) shows the graphs simulated by taking the values of  $\nu_m$  deduced from positions of the minima in Fig. 5(a). A good qualitative agreement with experimental data is evident, but due to the smearing effects related to light scattering the amplitude of modifications on the vertical axis is significantly lower in the experimental than in the theoretical curves, in particular at the lowest measured temperature.

Figure 6 summarizes the results on the evaluation of the grating strength  $\nu$  as a function of temperature. The values in different regions were obtained by different fitting procedures. For  $T > T_c$  the rocking curves were either fitted to Eq. (3) or evaluation of  $\nu$  via the method of the minima [Eq. (8)] was carried out. For  $T < T_c$  and the  $s$ -polarized beam, a fit corresponding to the angular broadening model was performed. For an  $s$ -polarized beam this is the only relevant method, because for  $\nu < \pi/2$  the positions of the minima in the  $\eta(\theta)$  are considerably shifted due to the smearing. For the  $p$ -polarized beam  $\nu > \pi/2$  and so also values deduced from the minima positions are relevant. For  $T > 55$  °C the agreement between the two methods is very good, while for  $T < 55$  °C the angular broadening model gives somewhat higher grating strengths. As both models are associated with several approximations, it is difficult to decide which of the obtained values are more realistic. However, as a steep jump of the grating strength  $\nu_p$  at 55 °C is difficult to explain, we believe that for our sample the minima method provides more realistic values than the broadening model.

To be able to judge the importance of light scattering phenomena at various temperatures, Fig. 7 gives the temperature dependence of the sum of detected intensities  $\langle I_\Sigma \rangle$  averaged over the measured angular span. In the isotropic phase the sample is practically transparent and therefore,  $\langle I_\Sigma \rangle \sim 1$ , while below  $T_c$  the values of  $\langle I_\Sigma \rangle$  monotonously decrease with decreasing temperature. The decrease for  $p$ -polarized light is around two times larger than for  $s$ -polarized light. At 42 °C nearly 90% of the incident power of the  $p$ -polarized radiation is scattered out from the detection directions, while the remaining 10% exhibit diffraction properties as shown in Fig. 2(b). This feature is not very suitable for practical purposes, but on the other hand it provides a wealthy resource of interesting phenomena related to light scattering in periodically mediated random media. The inset of Fig. 7 shows the detected effect of temperature on the broadening of the 0th diffraction order peak. In the isotropic phase the shape of the peak is practically equivalent to the unperturbed probe beam (Fig. 3), while in the nematic phase it is much broader. The broadening effect is attributed to light scattering.

Light scattering effects in periodic media are relatively rarely studied, and from this point of view HPDLCs repre-

sent unique materials in which diffraction effects due to periodically modulated scattering can be as high as the usual phase grating effects. On the other hand, in any real application, scattering should be minimized, which can be achieved by using smaller grating spacing  $\Lambda$  and consequently smaller droplet size. Scattering effects can be reduced also by decreasing the thickness of the sample. However, in this respect one should take into account that the validity of the two-beam coupling approximation (thick grating regime) [Eqs. (3), (5), and (6)] requires  $(L/\Lambda) > 10$  [53]. The main reason that we decided to study 50  $\mu\text{m}$  thick samples was a comparative investigation of their structural properties by SANS measurements, which will be reported in a separate paper. In addition to this we wanted to demonstrate various effects related to overmodulation of the grating strength which are usually overlooked.

A comparative analysis of the temperature dependencies of the 2nd and the 1st diffraction orders showed that in the isotropic phase the values of  $\nu_2$  are more than one order of magnitude lower than the values of  $\nu_1$ . In the nematic phase a ratio of  $\nu_2/\nu_1$  slowly increases with decreasing temperature, but it always remains below 0.2. This signifies that optical dielectric tensor modulation of our gratings is sinusoidal, which supports a description given by Eq. (4). The details of this study will be reported elsewhere.

Let us finally make an attempt to calculate the values of  $\varepsilon^0$  and  $\varepsilon^1$  [see Eq. (4)] for our grating. In the isotropic phase we obtained  $\nu_s = 1.89 \pm 0.03$ ,  $\nu_p = 1.84 \pm 0.03$ , and  $n_{0s} = n_{0p} = 1.52 \pm 0.01$ . From Eqs. (3)–(6) then it follows that  $\varepsilon_{yy}^0 = \varepsilon_{zz}^0 = 2.31 \pm 0.02$  and  $\varepsilon_{yy}^1 = \varepsilon_{zz}^1 = 0.032 \pm 0.001$ . The modulation  $\varepsilon^1$  is a consequence of the refractive-index mismatch between the polymer rich and the LC-rich regions. If one assumes that the LC-rich regions are composed only of the LC material and the fluoro-additive, then according to the volume fraction of the compounds the refractive index of these regions is expected to be  $n_{LCr} = 1.549$  (at  $\lambda = 598$  nm). On the other hand, if the polymer-rich regions were layers of a pure polymer their refractive index would be  $n_p = 1.473$ . The expected modulation for this extreme case is  $\varepsilon^1 = 0.115$ . The obtained 3.6 times lower value indicates that the ingredients of our sample are still quite far from being completely unmixed and separated into slices, which is in agreement with the profound light scattering and other observed phenomena.

In the nematic phase the obtained values of  $\varepsilon^0$ , which enter the fitting procedure mainly via the refraction law relating the values of  $\theta$  inside and outside of the sample, are more uncertain. For instance, at  $T = 42$  °C we find  $\varepsilon_{yy}^0 = 2.43 \pm 0.46$  (angular broadening model) and  $\varepsilon_{zz}^0 = 1.54 \pm 0.38$  (average value from the angular broadening and the minima model). Consequently, for the  $s$ -polarized beam associated with  $\nu_s = 0.86 \pm 0.08$  using Eq. (5) one obtains  $\varepsilon_{yy}^1 = 0.015 \pm 0.003$ . This reduced modulation with respect to the isotropic phase is attributed to the alignment of the LC material along the direction of the grating vector  $\mathbf{K}_g$ . For that reason the refractive index in the LC-rich regions for  $s$ -polarized light becomes governed by the value of  $n_\perp$  instead of the  $n_\parallel$ , so that a mismatch with the polymer-rich regions is lower. The effect on  $p$ -polarized light is the oppo-

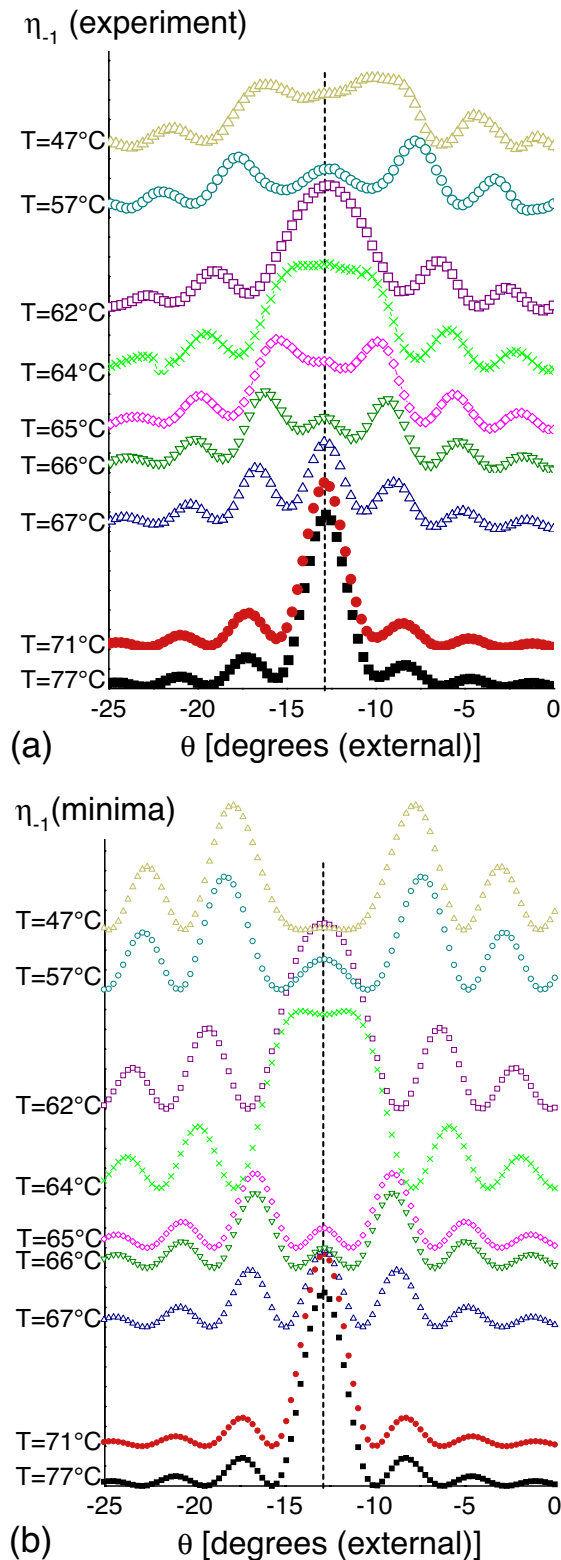


FIG. 5. (Color online) (a) Angular dependence of the measured 1st order diffraction efficiency  $\eta$  calculated according to Eq. (1) for  $p$ -polarized light at various temperatures. (b) Simulations of the associated MZ dependence using the values of the grating strengths as deduced from the positions of the minima in the experimental curves [Eq. (8)]. Vertical dashed lines denote the Bragg angle position.

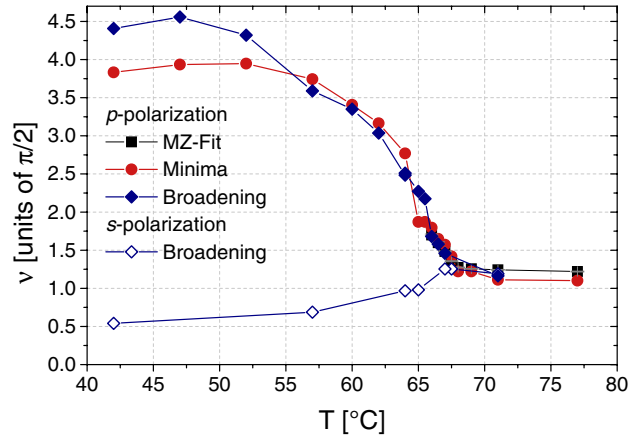


FIG. 6. (Color online) Temperature dependence of the grating strength for  $p$ -polarized (solid symbols) and for  $s$ -polarized (open symbols) light. The data were obtained from the fits to the MZ theory (squares) and from the fits to the angular broadening model (diamonds) or extrapolated from the positions of the minima in the rocking curves (circles).

site. In this case the extraordinary refractive index of the liquid crystal  $n_{\parallel}$  comes into play and therefore a mismatch with the polymer-rich regions is increased. From  $\nu_p = 6.44 \pm 0.47$  and Eq. (6) it follows  $\epsilon_{zz}^1 = 0.12 \pm 0.02$ .

In HPDLCs gratings the relations  $\epsilon_{xx}^0 \approx \epsilon_{yy}^0$  and  $\epsilon_{xx}^1 \approx \epsilon_{yy}^1$  are usually valid, which means that these media are more or less optically uniaxial [37,39]. Therefore the average optical anisotropy of the medium is given as  $n_a = n_{\parallel} - n_{\perp} = (\sqrt{\epsilon_{zz}^0} - \sqrt{\epsilon_{yy}^0})$ . Analogously one can define the modulation anisotropy

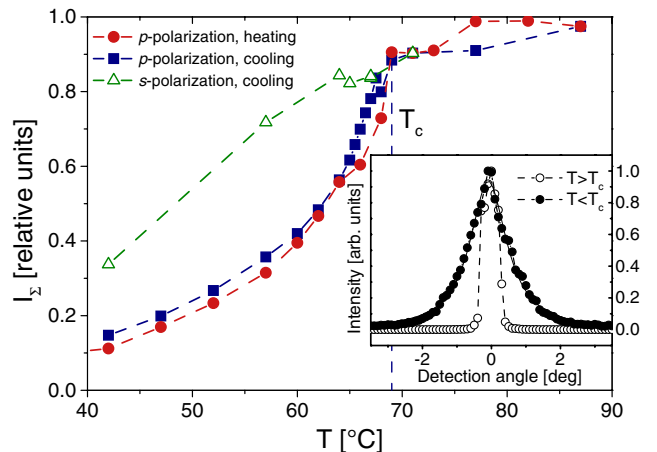


FIG. 7. (Color online) Temperature dependence of the sum of detected intensities for  $p$ -polarized (solid symbols) and for  $s$ -polarized (open symbols) light averaged over the angular span. Squares correspond to the data obtained during cooling and circles to the data obtained during heating. The inset shows angular spread of the 0th diffraction order in the isotropic and in the nematic phase measured by rotating the arm with the detector. For easier comparison the data are rescaled to the same maximal intensity.

$$n_{1,a} = n_{1,\parallel} - n_{1,\perp} = \frac{1}{2} \left( \frac{\varepsilon_{zz}^1}{\sqrt{\varepsilon_{zz}^0}} - \frac{\varepsilon_{yy}^1}{\sqrt{\varepsilon_{yy}^0}} \right). \quad (9)$$

In our experimental geometry  $n_{1,a}$  is practically proportional to the grating strength anisotropy, i.e., one can take  $n_{1,a} \approx (\lambda(\nu_p - \nu_s)/L\pi)$  [Eqs. (5) and (6)]. At  $T=42$  °C then it follows that  $n_{1,a}=0.031 \pm 0.003$ . This is about six times lower than the value of  $n_a$  for the pure LC compound at room temperature.

Because  $n_{1,a}$  is proportional to  $(\nu_p - \nu_s)$ , the main features of the temperature dependence of the  $n_{1,a}$  can be extracted simply from Fig. 6. One can notice that the graph in Fig. 6 reveals typical characteristics of the temperature dependence of the optical anisotropy  $n_a$  of the LC media. From this similarity we conclude that  $n_{1,a}$  is proportional to the optical anisotropy of the material forming the LC domains. Unfortunately this suggestion cannot be directly tested, because the medium within the LC domains is quite different from a pure LC material used for the mixture. This difference is evident from the considerable shift of the transition temperature and a strong increase of the viscoelastic constants as resolved from the DLS measurements.

As a warning against the conventional method to resolve the HPDLC anisotropy only from measurements of a difference between the diffraction efficiencies for  $p$ - and  $s$ -polarized beams at fixed orientation of the sample, we would like to point out the following properties of our sample. According to the usual definition of the diffraction efficiency [Eq. (1)], at  $T=42$  °C and in Bragg angle orientation, our grating has the diffraction efficiencies  $\eta_p(\theta_B) \sim 0.3$  and  $\eta_s(\theta_B) \sim 0.7$  [see Fig. 2(b)]. This observation would typically be associated with the opposite grating anisotropy as found from the corresponding values of  $\varepsilon^1$ . On the other hand, if one defines  $\eta$  as the ratio of  $I_{\pm 1}$  and the incident intensity, the values will decrease to  $\eta_p(\theta_B) \sim 0.04$  and  $\eta_s(\theta_B) \sim 0.2$ , while the associated anisotropy in favor of the  $s$ -polarized light will even increase. This is because light scattering effects are also strongly anisotropic. Even if the grating thickness  $L$  would be reduced to 10  $\mu\text{m}$ , the grating for the  $p$ -polarized case would remain overmodulated and a corresponding value of  $\eta_p/\eta_s$  would still be misleading.

#### IV. CONCLUSIONS

Our results show that above the nematic-isotropic phase transition temperature HPDLC media are optically isotropic. This indicates that the polymer matrix is isotropic, which means that no unidirectional ordering of the polymer molecules due to diffusive flow or stretching effects is developed

during the photopolymerization. Nonetheless, such an orientationally isotropic polymer network is able to induce a profound alignment of the LC domains in the nematic phase. As an isotropic polymer surface is associated with an azimuthally degenerated anchoring condition, the alignment cannot be explained only with the strong anchoring of the LC molecules in contact with the polymer filaments [4], but in addition, also a profound morphological anisotropy of the LC domains is necessary to support preferential orientation via the elastic forces.

The observed temperature dependence of the optical modulation anisotropy of our grating suggests that this anisotropy simply scales with the optical anisotropy of the material forming the LC domains. This signifies that the LC alignment, which is built up at the isotropic-nematic phase transition, does not exhibit any strong perturbations with decreasing temperature. However, because the LC alignment is not perfect, the increase of the LC anisotropy is associated with increase of light scattering. This is governed mostly by the mismatch of the LC orientation in neighboring domains. The scattering effects are coupled with the diffraction effects and for that reason a standard analysis of the grating properties is not applicable.

Our results show that for finite detection angles the observed rocking curves cannot be explained by simply adding a reduction factor to the standard description of the phase gratings. This is because light scattering produces not only a decrease of the light intensity, but also a profound angular smearing of the diffraction features. A more appropriate analysis can be made if one treats the scattering as a source of incoherent broadening of the angular span of the propagating waves. However, this rough approximation neglects holographic scattering phenomena and other coherent scattering effects. As a convenient simplification for the experimental analysis, we found that for partially smeared rocking curves some of the relevant parameters can be deduced if one focuses only on the positions of the minima in the rocking curves instead of fitting the entire curves. Although being very approximate, our models can serve as a basis for development of a more thorough theory of diffraction features of periodically modulated scattering media.

#### ACKNOWLEDGMENTS

We would like to acknowledge the financial support of the ÖAD in the frame of the STC program Slovenia-Austria (SI-A7/0405) and the Austrian Science Fund FWF (P-18988). One of us (I.D.-O.) is grateful for financial support from the Vienna University. We also thank E. Tillmanns for making one of his labs available to us.

- [1] T. J. Bunning, L. V. Natarjan, V. P. Tondiglia, and R. L. Sutherland, *Annu. Rev. Mater. Sci.* **30**, 83 (2000).  
 [2] G. P. Crawford, *Opt. Photonics News* **14**, 54 (2003).  
 [3] R. Jakubiak, T. J. Bunning, R. A. Vaia, L. V. Natarjan, and V. P. Tondiglia, *Adv. Mater. (Weinheim, Ger.)* **15**, 241 (2003).

- [4] K. K. Vardanyan, J. Qi, J. N. Eakin, M. De Sarkar, and G. P. Crawford, *Appl. Phys. Lett.* **81**, 4736 (2002).  
 [5] M. J. Escuti, J. Qi, and G. P. Crawford, *Opt. Lett.* **28**, 522 (2003).  
 [6] L. H. Domash, Y.-M. Chen, B. Gomatam, C. Gozewski, R. L.

- Sutherland, L. V. Natarajan, V. P. Tondiglia, T. J. Bunning, and W. W. Adams, *Proc. SPIE* **2689**, 188 (1996).
- [7] H. W. Ren, Y. H. Fan, and S. T. Wu, *Appl. Phys. Lett.* **83**, 1515 (2003).
- [8] L. V. Natarajan, R. L. Sutherland, V. P. Tondiglia, T. J. Bunning, and R. M. Neal, *Proc. SPIE* **3143**, 182 (1997).
- [9] D. E. Lucchetta, L. Criante, O. Francescangeli, and F. Simoni, *Mol. Cryst. Liq. Cryst.* **441**, 97 (2005).
- [10] T. G. Fiske, L. D. Silverstein, J. Colegrove, and H. Yuan, *SID Int. Symp. Digest Tech. Papers* **31**, 1134 (2000).
- [11] K. Tanaka, K. Kato, and M. Date, *Jpn. J. Appl. Phys., Part 1* **38**, 277 (1999).
- [12] C. C. Bowley and G. P. Crawford, *Appl. Phys. Lett.* **76**, 2235 (2000).
- [13] T. Kyu, D. Nwabunma, and H.-W. Chiu, *Phys. Rev. E* **63**, 061802 (2001).
- [14] S. Massenot, J. L. Kaiser, R. Chevallier, and Y. Renotte, *Appl. Opt.* **29**, 5489 (2004).
- [15] R. L. Sutherland, V. P. Tondiglia, L. V. Natarajan, and T. J. Bunning, *J. Appl. Phys.* **96**, 951 (2004).
- [16] T. J. Bunning, L. V. Natarajan, V. Tondiglia, R. L. Sutherland, D. L. Vezie, and W. W. Adams, *Polymer* **36**, 2699 (1995).
- [17] T. J. Bunning, L. V. Natarajan, V. P. Tondiglia, and R. L. Sutherland, *Polymer* **37**, 3147 (1996).
- [18] T. J. Bunning, L. V. Natarajan, V. P. Tondiglia, G. Dougherty, and R. L. Sutherland, *J. Polym. Sci., Part B: Polym. Phys.* **35**, 2825 (1997).
- [19] C. C. Bowley, H. J. Yuan, and G. P. Crawford, *Mol. Cryst. Liq. Cryst.* **331**, 2069 (1999).
- [20] R. T. Pogue, L. V. Natarajan, S. A. Siwecki, V. P. Tondiglia, R. L. Sutherland, and T. J. Bunning, *Polymer* **41**, 733 (2000).
- [21] K. K. Vardanyan, J. Qi, J. N. Eakin, M. De Sarkar, and G. P. Crawford, *Appl. Phys. Lett.* **81**, 4736 (2002).
- [22] M. Escuti, J. Qi, and G. P. Crawford, *Appl. Phys. Lett.* **83**, 1331 (2003).
- [23] M. De Sarkar, J. Qi, and G. P. Crawford, *Polymer* **43**, 7335 (2002).
- [24] M. De Sarkar, N. L. Gill, J. B. Whitehead, and G. P. Crawford, *Macromolecules* **36**, 630 (2003).
- [25] A. Y. G. Fuh, M. S. Tsai, T. C. Liu, and L. C. Chien, *Jpn. J. Appl. Phys., Part 1* **36**, 6839 (1997).
- [26] R. L. Sutherland, V. P. Tondiglia, L. V. Natarajan, T. J. Bunning, and W. W. Adams, *Appl. Phys. Lett.* **64**, 1074 (1994).
- [27] R. L. Sutherland, L. V. Natarajan, V. P. Tondiglia, T. J. Bunning, and W. W. Adams, *Proc. SPIE* **2152**, 303 (1994).
- [28] G. S. Iannacchione, D. Finotello, L. V. Natarajan, R. L. Sutherland, V. P. Tondiglia, T. J. Bunning, and W. W. Adams, *Europhys. Lett.* **36**, 425 (1996).
- [29] M. Jazbinšek, I. D. Olenik, M. Zgonik, A. K. Fontecchio, and G. P. Crawford, *J. Appl. Phys.* **90**, 3831 (2001).
- [30] M. E. Holmes and M. S. Malcuit, *Phys. Rev. E* **65**, 066603 (2002).
- [31] R. L. Sutherland, *J. Opt. Soc. Am. B* **19**, 2995 (2002).
- [32] R. L. Sutherland, L. V. Natarajan, V. P. Tondiglia, S. Chandra, C. K. Shepherd, D. M. Brandelik, S. A. Siwecki, and T. J. Bunning, *J. Opt. Soc. Am. B* **19**, 3004 (2002).
- [33] K. Kato, T. Hisaki, and M. Date, *Jpn. J. Appl. Phys., Part 1* **38**, 805 (1999).
- [34] J. J. Butler and M. S. Malcuit, *Opt. Lett.* **25**, 420 (2000).
- [35] J. J. Butler, M. S. Malcuit, and M. A. Rodriguez, *J. Opt. Soc. Am. B* **19**, 183 (2002).
- [36] D. E. Lucchetta, L. Criante, and F. Simoni, *J. Appl. Phys.* **93**, 9669 (2003).
- [37] D. E. Lucchetta, L. Criante, and F. Simoni, *Opt. Lett.* **28**, 725 (2003).
- [38] A. V. Galstyan, R. S. Hakobyan, S. Harbour, and T. Galstian, *Opt. Commun.* **241**, 23 (2004).
- [39] Y. Lu, F. Du, and S. T. Wu, *J. Appl. Phys.* **95**, 810 (2004).
- [40] S. Harbour, T. Galstian, R. S. Akopyan, and A. V. Galstyan, *Opt. Commun.* **238**, 261 (2004).
- [41] X. H. Sun, X. M. Tao, T. J. Ye, Y.-S. Szeto, and X. Y. Cheng, *J. Appl. Phys.* **98**, 043510 (2005).
- [42] R. L. Sutherland, L. V. Natarajan, V. P. Tondiglia, and T. J. Bunning, *Chem. Mater.* **5**, 1533 (1993).
- [43] F. Vita, A. Marino, V. Tkachenko, G. Abbate, D. E. Lucchetta, L. Criante, and F. Simoni, *Phys. Rev. E* **72**, 011702 (2005).
- [44] S. Meng, T. Kyu, L. V. Natarajan, V. P. Tondiglia, R. L. Sutherland, and T. J. Bunning, *Macromolecules* **38**, 4844 (2005).
- [45] R. L. Sutherland, V. P. Tondiglia, L. V. Natarajan, and T. J. Bunning, *Appl. Phys. Lett.* **79**, 1420 (2001).
- [46] R. L. Sutherland, *J. Opt. Soc. Am. B* **19**, 2995 (2002).
- [47] R. Caputo, A. V. Sukhov, C. Umeton, and R. F. Ushakov, *J. Exp. Theor. Phys.* **91**, 1190 (2000).
- [48] R. Caputo, L. De Sio, A. Veltri, C. Umeton, and A. V. Sukhov, *Opt. Lett.* **29**, 1261 (2004).
- [49] R. Caputo, A. Veltri, C. P. Umeton, and A. V. Sukhov, *J. Opt. Soc. Am. B* **21**, 1939 (2004).
- [50] A. d'Alessandro, R. Asquini, C. Gizzi, R. Caputo, C. Umeton, A. Veltri, and A. V. Sukhov, *Opt. Lett.* **29**, 1405 (2004).
- [51] T. Karasawa and Y. Taketomi, *Jpn. J. Appl. Phys., Part 1* **36**, 6388 (1997).
- [52] P. Hariharan, *Optical Holography: Principles, Techniques and Applications*, 2nd ed. (Cambridge University Press, Cambridge, England, 1996).
- [53] T. K. Gaylord and M. G. Moharam, *Appl. Opt.* **20**, 3271 (1981).
- [54] R. L. Sutherland, L. V. Natarajan, V. P. Tondiglia, T. J. Bunning, B. L. Epling, and D. M. Brandelik, *Proc. SPIE* **3010**, 142 (1997).
- [55] M. A. Ellabban, M. Fally, H. Uršič, and I. Drevenšek-Olenik, *Appl. Phys. Lett.* **87**, 151101 (2005).
- [56] H. Kogelnik, *Bell Syst. Tech. J.* **48**, 2909 (1969).
- [57] G. Montemezzani and M. Zgonik, *Phys. Rev. E* **55**, 1035 (1997).
- [58] I. Drevenšek-Olenik, M. Jazbinšek, M. Sousa, A. K. Fontecchio, G. P. Crawford, and M. Čopič, *Phys. Rev. E* **69**, 051703 (2004).
- [59] M. Jazbinšek, I. D. Olenik, M. Zgonik, A. K. Fontecchio, and G. P. Crawford, *Mol. Cryst. Liq. Cryst. Sci. Technol., Sect. A* **375**, 455 (2002).
- [60] A. Mertelj, L. Spindler, and M. Čopič, *Phys. Rev. E* **56**, 549 (1997).
- [61] M. Čopič and A. Mertelj, *Phys. Rev. Lett.* **80**, 1449 (1998).
- [62] V. K. S. Hsiao, T.-C. Lin, G. S. He, A. N. Cartwright, P. N. Prasad, L. V. Natarajan, V. P. Tondiglia, and T. J. Bunning, *Appl. Phys. Lett.* **86**, 131113 (2005).
- [63] J. T. Sheridan, *J. Mod. Opt.* **39**, 1709 (1992).